AJRCMB Articles in Press. Published on 29-October-2014 as 10.1165/rcmb.2014-0092OC

Guanylyl cyclase activation reverses resistive breathing-induced lung injury and inflammation

Constantinos Glynos[1,3], Dimitris Toumpanakis[1], Konstantinos Loverdos[1], Vassiliki Karavana[1], Zongmin Zhou[1], Christina Magkou[1], Maria Dettoraki[1], Fotis Perlikos[1], Athanasia Pavlidou[1], Vasilis Kotsikoris[3], Stavros Topouzis[3], Stamatios E. Theocharis[2], Peter Brouckaert[5,6], Athanassios Giannis[4], Andreas Papapetropoulos[1,3], and Theodoros Vassilakopoulos[1].

[1]George P. Livanos and Marianthi Simou Laboratories, Evangelismos Hospital, 1st Department of Pulmonary and Critical Care, University of Athens, Athens, Greece.
[2]Department of Pathology, University of Athens, Medical School, Athens, Greece.
[3]Laboratory of Molecular Pharmacology, Department of Pharmacy, University of Patras, Patras, Greece.
[4]Institut für Organische Chemie, Universität Leipzig, Leipzig, Germany.
[5]Department of Biomedical Molecular Biology, Ghent University, Ghent, Belgium.
[6]Department of Molecular Biomedical Research, VIB, Ghent, Belgium

Corresponding Author: T. Vassilakopoulos, MD, PhD
First Department of Critical Care, University of Athens Medical School, Evangelismos Hospital, 45–47 Ipsilandou Str, GR-10675 Athens, Greece.
E-mail: tvassil@med.uoa.gr

Conflict of interest: The authors have declared that no conflict of interest exists.

Running title: sGC activation reverses RB-induced lung injury

Author Contributions: Conception and design: C. G, A. P and T. V. Analysis, technical expertise and interpretation: C. G, D.T, K.L, V.K, Z.Z, Ch. M, M. D, F. P, V. Ko, Ath. P, S.E. T, A. P. and T. V. Research reagents, and critical review of the manuscript: A. P, S. T, A. G and P.B

This article has an online data supplement, which is accessible from this issue's table of content online at www.atsjournals.org

At a Glance Commentary

Scientific Knowledge on the Subject

Increased airway resistance during inspiration, triggers lung, diaphragm and systemic inflammation, alveolar-capillary barrier dysfunction, deranges respiratory mechanics and induces acute lung injury.

What This Study Adds to the Field

In previously healthy lungs increasing both the inspiratory and expiratory airway resistance, via tracheal banding induces lung barrier dysfunction and inflammation and downregulates the guanylyl cyclase expression. Pharmacological prevention or restoration of the decline of guanylyl cyclase pathway activity attenuates the resistive breathing induced lung injury, unravelling a potential therapeutic application in obstructive airway diseases.

AJRCMB Articles in Press. Published on 29-October-2014 as 10.1165/rcmb.2014-0092OC

Abstract

Rationale: Inspiratory resistive breathing (RB), encountered in obstructive lung diseases, induces lung injury. Soluble Guanylyl Cyclase (sGC)/cGMP pathway is downregulated in chronic and acute animal models of RB such as asthma, COPD and in endotoxin-induced acute lung injury. **Objectives**: i) To characterize the effects of increased concurrent inspiratory and expiratory resistance in mice, via tracheal banding, ii) To investigate the contribution of the sGC/cGMP pathway in in RB-induced lung injury. **Methods and Main Results**: Anesthetized C57BL/6 mice underwent RB achieved by restricting tracheal surface area to 50% (tracheal banding). RB for 24 hours resulted in increased bronchoalveolar lavage fluid cellularity and protein content, in marked leukocyte infiltration in the lungs and perturbed respiratory mechanics (increased tissue resistance and elasticity, shifted static pressure volume curve right and downwards, decreased static compliance), consistent with the presence of acute lung injury. RB downregulated the sGC expression in the lung. All manifestations of lung injury caused by RB were exacerbated by the administration of the sGC inhibitor, ODQ, or when RB was performed using sGC α1 knockout mice. Conversely, restoration of sGC signalling by prior administration of the sGC activator BAY 58-2667 prevented the RB-induced lung injury. Strikingly, direct pharmacological activation of sGC with BAY 58-2667 24h post-RB reversed, within 6 hours, the established lung injury. **Conclusions:** These findings raise the possibility that pharmacological targeting of the sGC/cGMP axis could be used to ameliorate lung dysfunction in obstructive lung diseases.

***Abstract Word Count*: 235**

Keywords: Lung Injury, Tracheal Banding, Soluble Guanylyl Cyclase.

INTRODUCTION

Acute increases in airway resistance (Acute Resistive Breathing (ARB) is encountered in many disease states such as asthma attacks, COPD exacerbations and upper airway obstruction. During ARB, strenuous contractions of the inspiratory muscles lead to large negative swings in the intrathoracic pressures that may induce injurious mechanical stress in resident lung cells. We have shown that increased airway resistance during inspiration increases alveolar-capillary membrane permeability, triggers lung inflammation, perturbs the mechanics of the respiratory system and induces acute lung injury in the lungs of previously healthy rats (1). However, in that model there was no expiratory resistance. It has been suggested that the presence of expiratory resistance with its accompanying intrinsic PEEP would oppose, during expiration, the forces producing pulmonary edema during inspiration secondary to the large negative intrathoracic pressures developed (2). We thus developed a murine-mouse model of ARB exhibiting both increased inspiratory and expiratory airway resistance, via tracheal banding. We hypothesized that increasing both the inspiratory and the expiratory airway resistance would cause injury to the lung, similar to purely inspiratory RB (1), on the premise that the structurally injurious processes during inspiration cannot be repaired or counteracted during expiration. The model of tracheal banding is most consistent with acute fixed upper airway obstruction, which is of course different than the obstructive patterns seen in COPD due to loss of alveoli and elasticity as well as the typically small airway constriction in asthma. In both of these disorders there is, in general, more difficulty with expiration than with inspiration. Having said that tracheal banding is the only way we are

AJRCMB Articles in Press. Published on 29-October-2014 as 10.1165/rcmb.2014-0092OC

aware of to acutely increase airway resistance without affecting the underlying airway inflammation (i.e. to induce pure mechanical acute resistive breathing).

Soluble Guanylyl Cyclase (sGC) mediates a wide range of physiological effects by catalyzing the conversion of GTP to cGMP (3). sGC is downregulated in animal models of both resistive breathing, such as COPD (4) or allergic asthma (5) and acute lung injury, such as endotoxin inhalation (6) or ischemia-reperfusion (7). Treatment of cultured cells with lipopolysaccharide, interleukin-1β, cytokine mixtures or uncontrolled production of NO and reactive oxygen species (ROS), decreases the mRNA stability and protein expression of both sGC subunits (α1 and β1), leading to sGC/cGMP pathway dysfunction (5, 6, 8, 9). In mice, TNF-α contributes to the downregulation of sGC expression in LPS-induced lung injury (6). Since cytokines and ROS -upregulated in the lung (1) and systemically (10, 11) during inspiratory RB- can reduce sGC expression, we hypothesised that RB would reduce sGC lung levels. Furthermore we investigated the functional role of sGC during RB, by activating the enzyme using BAY 58-2667, which protects the enzyme from proteolytic breakdown and reactivates cGMP production (12). We hypothesised that stabilization of sGC and restoration of its downstream signalling would ameliorate manifestations of acute lung injury due to RB.

METHODS

Methodological details are available in the online data supplement.

***Subjects*:** Eight-to-twelve-week old male C57BL/6 mice, were purchased from Pasteur Institute (Athens, Greece). sGC α1-/- mice, were provided by the SPF facility of the Department of Molecular Biomedical Research, VIB, Ghent, Belgium.

Tracheal Banding (RB) protocol: Anesthetized C57BL/6 mice underwent RB by placing surgically a sterile nylon band around the extrathoracic trachea restricting tracheal surface area to 50%. Sham surgery of control mice consisted of anesthesia, neck incision, and tracheal dissection without banding.

***Respiratory System Mechanics*:** Forced Oscillation Technique – i)Constant phase model, ii)Static Pressure Volume Curve. *R*espiratory system mechanics were estimated with the use of the forced oscillation technique and by performing static pressure volume curves (1).

Bronchoalveolar lavage (BAL) fluid: Bronchoalveolar lavage was performed, total and differential cell counts were obtained and protein content was estimated (6).

Lung Histology: The left lung was harvested and stained with hematoxylin-eosin. Lung histopathology was evaluated using a scoring system to grade the degree of inflammation(13).

cGMP measurements. cGMP production was measured in BALF, collected 24hrs after RB(4).

Quantitative real-time PCR. Total RNA was extracted from lungs, cDNA was synthesized and target and reference genes were measured by real-time PCR using custom designed primers(4).

Immunoblot analysis of sGC subunits: Samples of lung homogenates were subjected to SDS-PAGE and Western blotting. Values obtained for the α1 and β1 sGC subunit were normalized for actin and presented as % of control (4-6).

AJRCMB Articles in Press. Published on 29-October-2014 as 10.1165/rcmb.2014-0092OC

ODQ treatment: C57BL/6 mice were treated with inhaled ODQ (1H-[1, 2,4]oxodiazolo[4,3-]quinoxalin-l-one; 1 mg/mL: 5 mg ODQ diluted in 50μL DMSO and then further dissolved in 5 ml saline) or vehicle, 30 min before RB.

8pCPT cGMP treatment: C57BL/6 mice were treated with inhaled 8pCPT cGMP (2g/mL: 10 mg 8pCPT cGMP diluted in 50μL DMSO and then further dissolved in 5 ml saline) or vehicle, 30 min before RB.

BAY 58-2667 treatment: C57BL/6 mice were treated with the sGC activator BAY 58-2667 (10μg/kg, i.p.) or vehicle 30 min before (prophylactic protocol) or 24 hrs after RB (therapeutic protocol).

***Statistical analysis*:** Results are presented as means± SEM. ANOVA was performed with SPSS 11.5 software. Differences were considered significant when $p<0.05$.

RESULTS

RB via tracheal banding in wild type mice:

BALF protein and cell count. In RB mice with 50% reduction in tracheal surface area (see online supplement, Figure E1), BALF cellularity was increased compared to the control group, mainly due to macrophage influx (macrophages: 91% of total cell count) (Figure 1A). BALF protein content was increased after RB (Figure 1C). ***BALF cytokines.*** Acute RB increased BALF levels of TNF-α (Figure 1D), IL-6 (Figure 1E) and IL-1β(Figure 1F) in mice. ***Lung Histology***: RB increased interstitial and intraalveolar infiltration and focal thickening in the lung tissue (Figure 1G and H) and thus total lung injury score. ***Respiratory System Mechanics***: Tissue resistance and elasticity were increased after RB. RB shifted the static pressure volume curve right and downwards

consistent with the presence of lung injury. Accordingly, static compliance was decreased (Figure 1 I, J, and K).

Tracheal banding reduces the expression of soluble guanylyl cyclase

mRNA and Protein levels for the sGC subunits are decreased in the lungs of TB mice. After RB the mRNA levels of the sGC β1 subunit were reduced (Figure 2A). Western blotting analysis (Figure 2C) revealed that the expression of both the α1 and β1 protein subunits were reduced after RB (Figure 2D). ***cGMP measurement***: To determine whether attenuated sGC levels are reflected by impaired enzyme function after RB, we measured total cGMP levels in the BALF. RB resulted in reduced cGMP levels compared to controls (Figure 2B). Conversely, phosphodiesterase (PDE)-5, which hydrolyses cGMP to GMP, was increased after RB (Figure E3).

Inhibition of sGC activity by ODQ worsens RB-induced lung injury: To determine the effects of inhibition sGC activity during RB-induced acute lung injury, the sGC inhibitor ODQ was administered by inhalation 30min prior to RB (Figure 3). ***BALF protein and cell count***: Sham-operated animals treated with ODQ, did not increase BALF cellularity. In contrast, when ODQ was administered prior to RB, it increased BALF cellularity and protein content compared to the RB-only group (Figure 3A and B). ***Lung Histology***: The total lung injury score after RB was exacerbated by prior administration of ODQ (Figure 3C and D). ***Respiratory System Mechanics***: ODQ aggravated the effects of RB on airway resistance and tissue elasticity (Figure 3E and F).

AJRCMB Articles in Press. Published on 29-October-2014 as 10.1165/rcmb.2014-0092OC

sGC α1 deficiency in mice aggravates RB-induced lung injury. To determine the role of sGC downregulation in lung inflammation and respiratory system mechanics in our model, we compared sGCα1-/- and WT mice after tracheal banding. All basal parameters of lung injury and inflammation were similar between sham-operated WT and sGC α1-/- mice. ***BALF protein and cell count***: In sGCα1-/- mice, RB increased BALF cellularity mainly due to macrophages influx and aggravated barrier dysfunction, as reflected by the further increase in the BALF protein content, compared to WT mice (Figure 4A and B). ***Lung Histology***: sGC α1-/- mice subjected to RB exhibited increased interstitial and intraalveolar infiltration and focal thickening in the lung tissue compared to WT mice (Figure 4C and D). ***Respiratory System Mechanics***: sGCα1-/- mice exhibit exacerbated derangements of airway resistance and tissue elasticity after RB (Figure 4E and F).

Restoration of sGC downstream signalling: Activation of sGC using BAY 58-2667

A. Prophylactic administration of sGC activator BAY 58-2667 attenuated the RB-induced lung injury. To evaluate the protective effect of restoration of sGC downstream signalling, an NO-and heme independent sGC activator, BAY 58-2667 was administrated 30min prior to tracheal banding (Figure 5; schematic overview of the protocol in the Figure E6D). Prophylactic administration of BAY 58-2667 reversed the RB-induced attenuation of cGMP levels (see online supplement, Figure E5A). ***BALF protein and cell count***: BALF cellularity was increased after RB. Prophylactic administration of BAY 58-2667 reduced BALF cellularity (Figure 5A). BALF protein content was increased after RB compared to the sham operated group. Prophylactic administration of BAY 58-2667 reduced BALF protein content to control level (Figure 5B). ***Lung Histology***: Total

lung injury score was increased after RB, whereas prophylactic administration of BAY 58-2667, reduced interstitial and intraalveolar infiltration and focal thickening in the lung tissue, compared to RB mice (Figure 5C and D). ***Respiratory System Mechanics*****:** Prophylactic administration (i.p.) of BAY 58-2667 attenuated the effects of RB on airway resistance and tissue elasticity (Figure 5E and F).

B. ***Therapeutic administration of sGC activator BAY 58-2667 attenuated the RB-induced lung injury.*** To test a putative therapeutic effect of the sGC activation, BAY 58-2667, was administrated i.p., 24 hrs after tracheal banding and mice were euthanized 6h after BAY administration (schematic overview of the protocol in E6D). Therapeutic administration of BAY 58-2667 reversed the RB-induced attenuation of cGMP levels (see online supplement, Figure E5B). ***BALF protein and cell count***: Therapeutic treatment of mice with BAY 58-2667 reversed the increases in BALF cellularity induced by RB to control levels (Figure 6A). However, this treatment did not reverse the compromise of the barrier function, since it had no effect the increase in BALF protein content evoked by RB (Figure 8B). ***Lung Histology***: Therapeutic administration of BAY 58-2667, reduced interstitial and intraalveolar infiltration and focal thickening in the lung tissue, compared to RB mice (Figure 6C and D). ***Respiratory System Mechanics*****:** Therapeutic administration of BAY 58-2667 attenuated the effect of RB on airway resistance and tissue elasticity. (Figure 6E and F).

DISCUSSION

The major findings are: 1) concurrent inspiratory and expiratory RB (via tracheal banding) induces acute lung injury in mice; 2) RB induces downregulation of sGC; 3)

AJRCMB Articles in Press. Published on 29-October-2014 as 10.1165/rcmb.2014-0092OC

pharmacological inhibition or genetic ablation of the sGC aggravates the RB-induced lung injury; 4) pharmacological rescue of the guanylyl cyclase signalling dysfunction, using a sGC activator (BAY 58-2667), attenuates the RB-induced lung injury; 5) stabilization of sGG by administration of BAY 58-2667 after the establishment of lung injury, reverses RB-induced lung injury.

Strenuous inspiratory RB in healthy humans induces plasma IL-1β, IL-6 and TNF-α, initiating a systemic inflammatory response (10, 11). Inspiratory RB in rats increases alveolar-capillary membrane permeability, induces lung inflammation and perturbs respiratory system mechanics, culminating in acute lung injury (1). In both the animal and the human models there was no expiratory resistance, contrary to what is observed in asthma attacks, COPD exacerbations or cases of upper airway obstruction. It has been suggested that the presence of expiratory resistance with its accompanying intrinsic PEEP would prevent pulmonary edema development (2).

We thus developed a mouse model of resistive breathing which exhibits increased both inspiratory and expiratory airway resistance, via tracheal banding. We studied mice for two reasons: to determine whether our previous findings were species-specific and to establish a clinically relevant model of RB in mice, which allows for the study of genetically engineered animals.

Acute RB for 24 hours increased BALF cellularity mainly due to an increase in macrophages, consistent with acute inflammation. In addition, lung histology revealed patchy areas of inflammatory cell recruitment, alveolar hemorrhage, intra-alveolar and interstitial edema. The pro-inflammatory cytokines TNF-α, IL-6 or IL-1β were also

elevated in the BALF. These might originate from infiltrating leukocytes and/or might be produced from cells resident in the lung via "mechanotransduction" or in response to other locally produced stimuli. Acute RB in mice was followed by increased tissue elasticity and resistance and downward shift of the pressure-volume curve. Accordingly, static compliance was decreased. These alterations are well described in acute lung injury and elasticity increases have been previously correlated with lung injury (1, 14, 15). Thus, the presence of expiratory resistance did not prevent lung injury, probably because the structurally injurious processes in the lung during inspiration can not be repaired or counteracted during expiration.

The current findings in mice, combined with our recent ones in rats, suggest that the RB-induced lung injury is not species-specific. One might wonder whether the degree of airway narrowing in our model was excessive or was within the pathophysiologically relevant range. The negligible mortality of both wild type and transgenic mice after tracheal banding clearly allows this technique developed in our laboratory, to be used for acute experiments in both normal and genetically engineered mice, provided that, similar to our knock-out murine line (sGCa1 -/-), they do not already exhibit increased baseline inflammation and respiratory dysfunction. We still need to investigate whether this approach can be used with murine lines that have compromised respiratory function.

RB resulted in the attenuation of the sGC/cGMP signal cascade. After 24hrs of tracheal banding, mRNA levels of the sGCβ1 subunit were drastically reduced. As sGC is an obligate heterodimer, decreased levels of β1 subunit indicate a decline in the amount of the active enzyme (16). Western blot analyses revealed that both α1 and β1 subunits

AJRCMB Articles in Press. Published on 29-October-2014 as 10.1165/rcmb.2014-0092OC

were reduced after 24 hours of RB. Moreover, phosphodiesterase-5 (PDE-5), which hydrolyses cGMP to GMP, terminating its action, was increased with RB, further impairing sGC/cGMP downstream pathway, in agreement to our previous findings in mice exposed to cigarette smoke (4). Our model of RB distinguishes the mechanotransductive effect of the increased airway resistance (i.e. tracheal banding in previously healthy lungs, the mechanical stressor) on sGC signalling from the underlying airway inflammation of obstructive airway diseases (i.e asthma and COPD which also have increased airway resistance, yet with pre-existing underlying airway inflammation). This is the first time that downregulation of sGC expression is shown in the lung secondary to the mechanotransductive effect of RB.

Treatment of cultured cells with inflammatory stimuli attenuates the sGC mRNA stability or protein expression (17-20). Increased inflammation and TNF-α, IL-6 or IL-1β upregulation was documented in the BALF of mice after RB. However, an alternative explanation for the reduction of the sGC levels that is not mutually exclusive with the increase in cytokines is mechanotransduction, i.e. increased mechanical stress on the resident lung cells due to the large negative intrathoracic pressures developed.

Oxidative stress along with inflammatory stimuli could impair sGC signalling due to acute RB. We treated animals with ODQ, an agent that selectively oxidizes sGC prior to RB. This resulted in augmented inflammation, vascular leakage and mechanical derangements. Our data is consistent with a previous study of endotoxin induced-lung injury where oxidation of sGC and further attenuation of its enzymatic activity using ODQ caused increased inflammation and vascular leakage (21). In support of this hypothesis, we have previously observed that inhibition of sGC by ODQ was

accompanied by more pronounced bronchial responsiveness in an asthma model (5) and lung barrier dysfunction in the LPS-induced lung injury model (6). We investigated the role of sGC downstream signalling in RB-induced lung injury using sGCα1 knock-out mice subjected to tracheal banding. In these adult sGCα1 knock-out mice sGC β1 subunit lung levels are decreased (22). RB-induced lung injury was more pronounced when sGC/cGMP signalling was impaired due to sGCα1 subunit knock-out, reinforcing the notion that sGC signalling protects lung integrity. Interestingly, no difference in BALF cellularity, protein content or mechanical properties was observed between sham operated wild type and sGCα1 knockout mice. It seems that at basal conditions in uninjured animals the α2β1 isoform of the sGC is able to maintain downstream signalling pathways. However, during RB via tracheal banding, sGC α1β1 appeared to play a crucial role.

To elucidate the effect of sGC activity in RB-induced lung injury, wild type mice were treated with the heme- and NO-independent sGC activator BAY 58-2667 30 minutes before tracheal banding (prophylactic protocol). Prophylactic administration of BAY 58-2667 preferentially protects against diseases characterized by marked oxidative injury, such as pulmonary hypertension (23) or cardiovascular diseases (24, 25) by activating the NO-insensitive, oxidized form of sGC. We observed that prophylactic administration of BAY 58-2667 attenuated the RB-induced lung injury by reducing to control levels the BALF cellularity and protein content, and improving airway resistance and tissue elasticity.

AJRCMB Articles in Press. Published on 29-October-2014 as 10.1165/rcmb.2014-0092OC

To investigate the functional role of the sGC downstream signalling, a cGMP analogue (8pCPTcGMP) was administered prior to RB. PKG activation by 8pCPTcGMP attenuated the RB-induced increase in BALF cellularity and protein content (see online supplement, Figure E3). The elevated cytokine response to RB was almost abolished after inhalation of 8pCPTcGMP (see online supplement, Figure E4). Lung mechanics perturbation was also entirely prevented (see online supplement, Figure E3). Since restoring sGC downstream signalling by 8pCPTcGMP administration attenuated the lung injury caused by RB, we propose that downregulation of sGC is causally related to the observed lung injury rather than the result of it.

To investigate whether restoration of sGC/cGMP signalling could be effective in a clinically meaningful manner, we administered BAY 58-2667 after 24 hours of tracheal banding, when injury is well-established and examined the animals 6 hours later (therapeutic protocol). Strikingly, therapeutic administration of BAY 58-2667 reversed the RB-induced lung injury, attenuated BALF cellularity and improved the mechanical parameters. Thus, guanylyl cyclase exerts a causative role in the pathological alterations and mechanical derangements in our model of RB, and restoration of its activity has therapeutic potential.

The protective effect of sGC signalling in our RB model is consistent with observations on the endothelial barrier (21). The sGC stimulator BAY 41-2272 reduces the elevated leukocyte rolling and adhesion in the capillaries of eNOS -/- mice (26). sGC stimulation inhibits the IL-1β-induced increase in leukocyte adhesion by attenuating P-selectin expression (26). Increasing intracellular cGMP, by 8pCPT-cGMP administration,

attenuated cell death and evidence of cytotoxicity in H_2O_2-challenged mouse lung microvascular endothelial cell monolayers and ROS-injured isolated perfused mouse lungs, respectively (27). Post-treatment with the sGC activator BAY 58-2667 in a mouse model of endotoxic shock reduced hypothermia and IL-6 levels, and attenuated cardiomyocyte apoptosis, heart rate and mortality (28). Such effects of sGC signalling could also be mediating the protective role of the sGC in the RB-induced lung injury.

In summary, we have shown RB induces downregulation of the sGC in the lung and acute lung injury. Pharmacological restoration of the sGC/cGMP pathway reverses the observed lung injury. Our results open the interesting possibility that sGC stimulation can be used in clinical conditions of severe RB i.e asthma attacks and COPD exacerbations. sGC stimulators have been successfully used in patients with chronic thromboembolic pulmonary hypertension and pulmonary arterial hypertension (29, 30). Our current findings and the findings of our previous study (4) suggest that sGC signalling restoration is worth investigating in both stable and exacerbated obstructive lung diseases.

Acknowledgements

The authors would like to thank Mrs. Zoi Kollia and Tatiana Michailidou for technical assistance with experimental procedures. This work was funded by the Aristia grant of the GSRT to T.V., the Hellenic Thoracic Society grant to C.G. and A.P. The authors A.P. S.T and P.B. are supported by the COST Action BM1005 (European Network on

AJRCMB Articles in Press. Published on 29-October-2014 as 10.1165/rcmb.2014-0092OC

Gasotransmitters). The authors C.G. and V.K. were supported by EU grant (Call: FP7-REGPOT2011-1): "establishment of a centre of excellence for structured-based drug target characterization: strengthening the research capacity of South-Eastern Europe" (SEE-DRUG, www.seedrug.upatras.gr).

FIGURES

Figure 1: ***Tracheal banding induces lung injury.*** **A**.Tracheal banding induces inflammatory cells influx in the BALF. Total cells and macrophages in BALF of TB mice are increased compared to sham operated mice (control) following 24 hours of resistive breathing. **B**. Neutrophils, lymphocytes and eosinophils (B1) influx in BALF of TB mice. **C.** Tracheal banding increases BALF protein concentration. Tracheal banding increases BALF concentration of cytokines : **D.** TNF-α. **E.** Interleukin-6 **F.** Intereleukin-1β. **G.** Lung histological evaluation by light microscopy revealed the existence of neutrophil infiltration in mice 24 hours after tracheal banding. RB increases interstitial and intraalveolar infiltration and focal congestion in the lung tissue. **H.** Representative histological section stained with hematoxylin-eosin of quietly breathing (control) and treated mice, after tracheal banding, respectively. Note that, following 24 hours of tracheal banding, intra-alveolar and interstitial infiltration of inflammatory cells, focal thickening and capillary congestion occur.

Respiratory System Mechanics: **I.** Tissue resistance by force oscillation technique is elevated following tracheal banding. **J.** Tissue elasticity is elevated following tracheal banding. **K**. Static compliance of the respiratory system was decreased 24 hours after

tracheal banding. Values are expressed as means ± SEM; n=10; *p< 0.05 from sham operated (control) group.

Figure 2: ***The expression of sGC is decreased in the lungs of TB mice*. A.** cDNA samples from total RNA of sGCα1 and β1 subunits, extracted from homogenized mice lung were used and PCR amplifications were performed in triplicate. 18S and GAPDH amplification was used as the endogenous control. **B.** RB decreased cGMP production in BALF collected 24 hours after tracheal banding **C.** Protein levels of sGC subunits are decreased in mice after 24 hours of resistive breathing. Sham operated (control) or TB (TB) mice were sacrificed 24hours after treatment. Representative western blots for the α-1, β-1 and β-actin. **D.** Blots were quantified by densitometry. Expression for each subunit normalized for β-actin was set at 100% for sham operated mice. Values are expressed as means ± SEM; n=10; *p< 0.05 from sham operated (control) group.

Figure 3: ***Inhibition of sGC activity by ODQ worsens RB-induced lung injury***. **A.** Exposure of animals to the nebulised ODQ, aggravates the effect of tracheal banding by increasing BALF inflammatory cell number. **B.** ODQ inhalation worsens the effect of tracheal banding on albumin leakage.

ODQ aggravates lung histopathology after tracheal banding. **C.** Lung histological evaluation by light microscopy revealed a worse inflammation and neutrophil infiltration in TB mice treated with ODQ compared to the TB group. Inhalation of ODQ increased interstitial and intraalveolar infiltration and focal congestion in the lung tissue, compared to the TB group. **D.** Representative histological section stained with hematoxylin-eosin of

AJRCMB Articles in Press. Published on 29-October-2014 as 10.1165/rcmb.2014-0092OC

quietly breathing (control) and TB (TB) mice, with or without exposure to ODQ, respectively.

ODQ aggravates lung mechanics after tracheal banding **E.** Elevated tissue elasticity, following tracheal banding, was further increased after inhalation of ODQ. **F.** The decrease of the static compliance of the respiratory system, 24hs after tracheal banding was further attenuated after inhalation of ODQ. Values are expressed as means ± SEM; n=10; *p< 0.05 from sham operated (control) group and # p<0.05 from TB group.

Figure 4: ***sGC α1 deficiency in mice aggravates lung injury caused by tracheal banding (TB).*** **A.** sGC α1-/- mice subjected to tracheal banding, aggravates the effect of TB by increasing BALF inflammatory cell number. **B.** sGC α1 deficiency worsens the effect of tracheal banding on albumin leakage. **C.** Lung histological evaluation by light microscopy in sGC α1-/- and WT mice subjected to TB. **D.** Representative histological section stained with hematoxylin-eosin of quietly breathing (control) and TB sGC α1-/- and WT mice. **E.** Elevated tissue elasticity, following tracheal banding, was further increased in sGC α1-/-. **F.** The decrease of the static compliance of the respiratory system, 24 hourss after tracheal banding was further attenuated in sGC α1-/-. Values are expressed as means ± SEM; n=8; *p< 0.05 from sham operated (control) group and # p<0.05 from TB group of WT mice.

Figure 5. ***Activation of sGC attenuates lung injury caused by tracheal banding-Prophylactic protocol.*** **A.** Administration (i.p.) of BAY 58-2667 30min prior to tracheal

banding, reversed the effect of RB by reducing BALF inflammatory cell number. **B.** BAY 58-2667 attenuated the effect of RB on albumin leakage.

Activation of sGC improves lung histopathology after tracheal banding.**C.** Lung histological evaluation by light microscopy revealed the attenuation of inflammation and neutrophil infiltration in mice treated with BAY 58-2667 prior to tracheal banding. BAY 58-2667 decreased interstitial and intraalveolar infiltration and focal congestion in the lung tissue, compared to the group of TB (TB) mice. **D.** Representative histological section stained with hematoxylin-eosin of quietly breathing and TB (TB) mice, with or without BAY 58-2667, respectively. Note that intralveolar and interstitial infiltration of inflammatory cells, focal thickening and capillary congestion that occurs following tracheal banding, is attenuated when BAY 58-2667 is administrated prior to TB.

Activation of sGC improves lung mechanics after tracheal banding. **E.** Elevated airway resistance and **F.** tissue elasticity, following tracheal banding, was attenuated when BAY 58-2667 was administrated prior to TB**.** Values are expressed as means ± SEM; n=10; *p< 0.05 from sham operated (control) group and # p<0.05 from TB group.

Figure 6: ***Therapeutic activation of sGC attenuates lung injury caused by tracheal banding-Therapeutic protocol*** **A.** Administration (i.p.) of BAY 58-2667 24 hrs after tracheal banding reversed the effect of RB by reducing BALF inflammatory cell number. **B.** BAY 58-2667 attenuated the effect of RB on albumin leakage.

Activation of sGC improves lung histopathology after tracheal banding. **C.** Lung histological evaluation by light microscopy revealed the attenuation of inflammation and neutrophil infiltration in mice treated with BAY 58-2667. BAY 58-2667 decreased

AJRCMB Articles in Press. Published on 29-October-2014 as 10.1165/rcmb.2014-0092OC

interstitial and intraalveolar infiltration and focal congestion in the lung tissue, compared to the group of TB (TB) mice. **D.** Representative histological section stained with hematoxylin-eosin of quietly breathing and TB (TB) mice, with or without BAY 58-2667, respectively. Note that intralveolar and interstitial infiltration of inflammatory cells, focal thickening and capillary congestion that occurs following tracheal banding, is attenuated when BAY 58-2667 is administrated 24hrs after TB.

Activation of sGC improves lung mechanics after tracheal banding. **E.** Elevated airway resistance and **F.** tissue elasticity, following tracheal banding, was attenuated when BAY 58-2667 was administrated after TB**.** Values are expressed as means ± SEM; n=10; *p< 0.05 from sham operated (control) group and # p<0.05 from TB group.

Figure 7: ***A schematic overview of the RB-induced lung injury***. Resistive breathing (RB) increased (↑) IL-6, TNF-α and IL-1β in the BALF. In the lung tissue RB reduced expression (↓) of soluble guanylyl cyclase (sGC) followed by reduced (↓) cyclic guanosine monophosphate (cGMP) generation and reduced cGMP-dependent protein kinase (PKG) function as reflected by attenuation of lung injury using a PKG activator, 8pCPTcGMP. The sGC downstream signalling is mainly determined by phosphodiesterases (PDE)-5A which hydrolyses cGMP to GMP, in a negative feed-back regulation. The impaired sGC/cGMP/PKG signalling pathway contributes to lung injury as reflected by elevated BAL cellularity, protein and cytokine content, pathological evaluation and derangement of respiratory system mechanics. Administration of BAY 58-2667 activated sGC and attenuated lung injury due to resistive breathing.

Reference List

1. Toumpanakis D, Kastis GA, Zacharatos P, Sigala I, Michailidou T, Kouvela M, Glynos C, Divangahi M, Roussos C, Theocharis SE, et al. Inspiratory Resistive Breathing Induces Acute Lung Injury. *Am J Respir Crit Care Med* 2010;182:1129-1136.

2. Willms D, Shure D. Pulmonary Edema Due to Upper Airway Obstruction in Adults. *Chest* 1988;94:1090-1092.

3. Friebe A, Koesling D. Regulation of Nitric Oxide-Sensitive Guanylyl Cyclase. *Circ Res* 2003;93:96-105.

4. Glynos C, Dupont LL, Vassilakopoulos T, Papapetropoulos A, Brouckaert P, Giannis A, Joos GF, Bracke KR, Brusselle GG. The Role of Soluble Guanylyl Cyclase in Chronic Obstructive Pulmonary Disease. *Am J Respir Crit Care Med* 2013;188:789-799.

5. Papapetropoulos A, Simoes DC, Xanthou G, Roussos C, Gratziou C. Soluble Guanylyl Cyclase Expression Is Reduced in Allergic Asthma. *Am J Physiol Lung Cell Mol Physiol* 2006;290:L179-L184.

6. Glynos C, Kotanidou A, Orfanos SE, Zhou Z, Simoes DC, Magkou C, Roussos C, Papapetropoulos A. Soluble Guanylyl Cyclase Expression Is Reduced in LPS-

AJRCMB Articles in Press. Published on 29-October-2014 as 10.1165/rcmb.2014-0092OC

Induced Lung Injury. *Am J Physiol Regul Integr Comp Physiol* 2007;292:R1448-R1455.

7. Egemnazarov B, Sydykov A, Schermuly RT, Weissmann N, Stasch JP, Sarybaev AS, Seeger W, Grimminger F, Ghofrani HA. Novel Soluble Guanylyl Cyclase Stimulator BAY 41-2272 Attenuates Ischemia-Reperfusion-Induced Lung Injury. *Am J Physiol Lung Cell Mol Physiol* 2009;296:L462-L469.

8. Gerassimou C, Kotanidou A, Zhou Z, Simoes DC, Roussos C, Papapetropoulos A. Regulation of the Expression of Soluble Guanylyl Cyclase by Reactive Oxygen Species. *Br J Pharmacol* 2007;150:1084-1091.

9. Pyriochou A, Beis D, Koika V, Potytarchou C, Papadimitriou E, Zhou Z, Papapetropoulos A. Soluble Guanylyl Cyclase Activation Promotes Angiogenesis. *J Pharmacol Exp Ther* 2006;319:663-671.

10. Vassilakopoulos T, Zakynthinos S, Roussos C. Strenuous Resistive Breathing Induces Proinflammatory Cytokines and Stimulates the HPA Axis in Humans. *Am J Physiol* 1999;277:R1013-R1019.

11. Vassilakopoulos T, Katsaounou P, Karatza MH, Kollintza A, Zakynthinos S, Roussos C. Strenuous Resistive Breathing Induces Plasma Cytokines: Role of Antioxidants and Monocytes. *Am J Respir Crit Care Med* 2002;166:1572-1578.

12. Evgenov OV, Pacher P, Schmidt PM, Hasko G, Schmidt HH, Stasch JP. NO-Independent Stimulators and Activators of Soluble Guanylate Cyclase: Discovery and Therapeutic Potential. *Nat Rev Drug Discov* 2006;5:755-768.

13. Murao Y, Loomis W, Wolf P, Hoyt DB, Junger WG. Effect of Dose of Hypertonic Saline on Its Potential to Prevent Lung Tissue Damage in a Mouse Model of Hemorrhagic Shock. *Shock* 2003;20:29-34.

14. Allen G, Bates JH. Dynamic Mechanical Consequences of Deep Inflation in Mice Depend on Type and Degree of Lung Injury. *J Appl Physiol* 2004;96:293-300.

15. Harris RS. Pressure-Volume Curves of the Respiratory System. *Respir Care* 2005;50:78-98.

16. Buechler WA, Nakane M, Murad F. Expression of Soluble Guanylate Cyclase Activity Requires Both Enzyme Subunits. *Biochem Biophys Res Commun* 1991;174:351-357.

17. Filippov G, Bloch DB, Bloch KD. Nitric Oxide Decreases Stability of MRNAs Encoding Soluble Guanylate Cyclase Subunits in Rat Pulmonary Artery Smooth Muscle Cells. *J Clin Invest* 1997;100:942-948.

18. Papapetropoulos A, Abou-Mohamed G, Marczin N, Murad F, Caldwell RW, Catravas JD. Downregulation of Nitrovasodilator-Induced Cyclic GMP Accumulation in Cells Exposed to Endotoxin or Interleukin-1 Beta. *Br J Pharmacol* 1996;118:1359-1366.

AJRCMB Articles in Press. Published on 29-October-2014 as 10.1165/rcmb.2014-0092OC

19. Papapetropoulos A, Go CY, Murad F, Catravas JD. Mechanisms of Tolerance to Sodium Nitroprusside in Rat Cultured Aortic Smooth Muscle Cells. *Br J Pharmacol* 1996;117:147-155.

20. Takata M, Filippov G, Liu H, Ichinose F, Janssens S, Bloch DB, Bloch KD. Cytokines Decrease SGC in Pulmonary Artery Smooth Muscle Cells Via NO-Dependent and NO-Independent Mechanisms. *Am J Physiol Lung Cell Mol Physiol* 2001;280:L272-L278.

21. Mehta S. The Effects of Nitric Oxide in Acute Lung Injury. *Vascul Pharmacol* 2005;43:390-403.

22. Buys ES, Sips P, Vermeersch P, Raher MJ, Rogge E, Ichinose F, Dewerchin M, Bloch KD, Janssens S, Brouckaert P. Gender-Specific Hypertension and Responsiveness to Nitric Oxide in SGCalpha1 Knockout Mice. *Cardiovasc Res* 2008;79:179-186.

23. Chester M, Seedorf G, Tourneux P, Gien J, Tseng N, Grover T, Wright J, Stasch JP, Abman SH. Cinaciguat, a Soluble Guanylate Cyclase Activator, Augments CGMP After Oxidative Stress and Causes Pulmonary Vasodilation in Neonatal Pulmonary Hypertension. *Am J Physiol Lung Cell Mol Physiol* 2011;301:L755-L764.

24. Stasch JP, Schmidt PM, Nedvetsky PI, Nedvetskaya TY, AK HS, Meurer S, Deile M, Taye A, Knorr A, Lapp H, et al. Targeting the Heme-Oxidized Nitric Oxide Receptor for Selective Vasodilatation of Diseased Blood Vessels. *J Clin Invest* 2006;116:2552-2561.

25. Stasch JP, Pacher P, Evgenov OV. Soluble Guanylate Cyclase As an Emerging Therapeutic Target in Cardiopulmonary Disease. *Circulation* 2011;123:2263-2273.

26. Ahluwalia A, Foster P, Scotland RS, McLean PG, Mathur A, Perretti M, Moncada S, Hobbs AJ. Antiinflammatory Activity of Soluble Guanylate Cyclase: CGMP-Dependent Down-Regulation of P-Selectin Expression and Leukocyte Recruitment. *Proc Natl Acad Sci U S A* 2004;101:1386-1391.

27. Stephens RS, Rentsendorj O, Servinsky LE, Moldobaeva A, Damico R, Pearse DB. CGMP Increases Antioxidant Function and Attenuates Oxidant Cell Death in Mouse Lung Microvascular Endothelial Cells by a Protein Kinase G-Dependent Mechanism. *Am J Physiol Lung Cell Mol Physiol* 2010;299:L323-L333.

28. Vandendriessche B, Rogge E, Goossens V, Vandenabeele P, Stasch JP, Brouckaert P, Cauwels A. The Soluble Guanylate Cyclase Activator BAY 58-2667 Protects Against Morbidity and Mortality in Endotoxic Shock by Recoupling Organ Systems. *PLoS One* 2013;8:e72155.

29. Ghofrani HA, D'Armini AM, Grimminger F, Hoeper MM, Jansa P, Kim NH, Mayer E, Simonneau G, Wilkins MR, Fritsch A, et al. Riociguat for the Treatment of Chronic Thromboembolic Pulmonary Hypertension. *N Engl J Med* 2013;369:319-329.

30. Ghofrani HA, Galie N, Grimminger F, Grunig E, Humbert M, Jing ZC, Keogh AM, Langleben D, Kilama MO, Fritsch A, et al. Riociguat for the Treatment of Pulmonary Arterial Hypertension. *N Engl J Med* 2013;369:330-340.

AJRCMB Articles in Press. Published on 29-October-2014 as 10.1165/rcmb.2014-0092OC

Figure 1

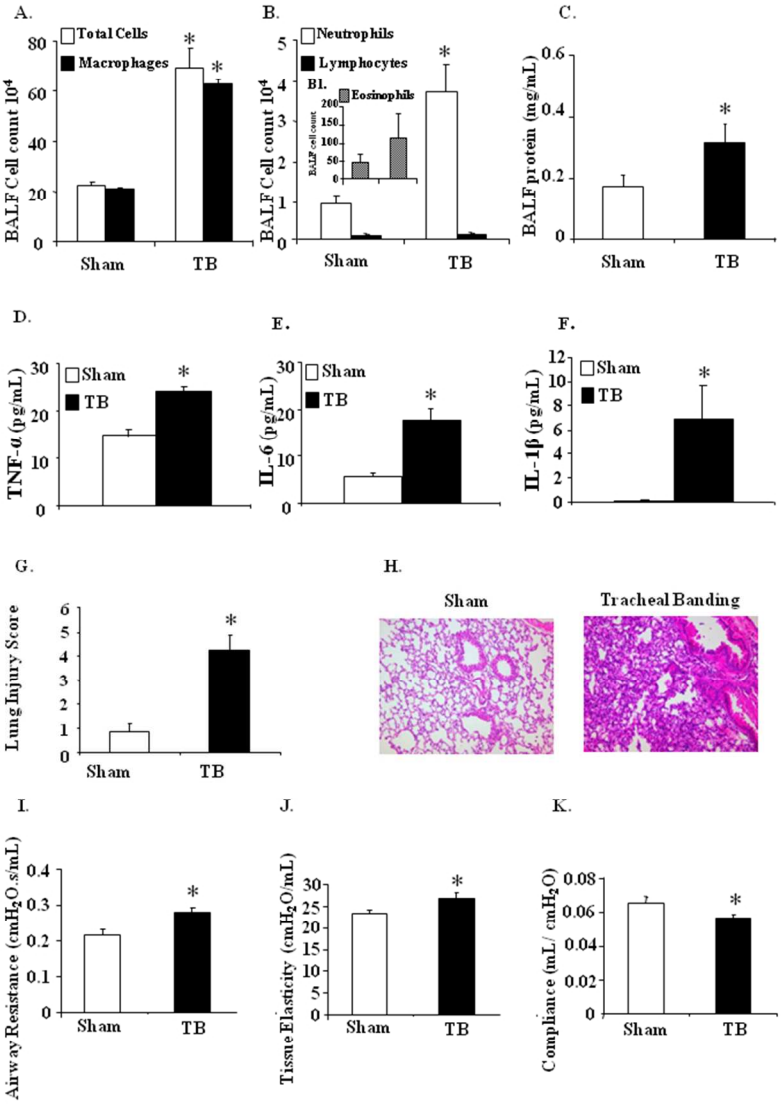

190x275mm (96 x 96 DPI)

Figure 2

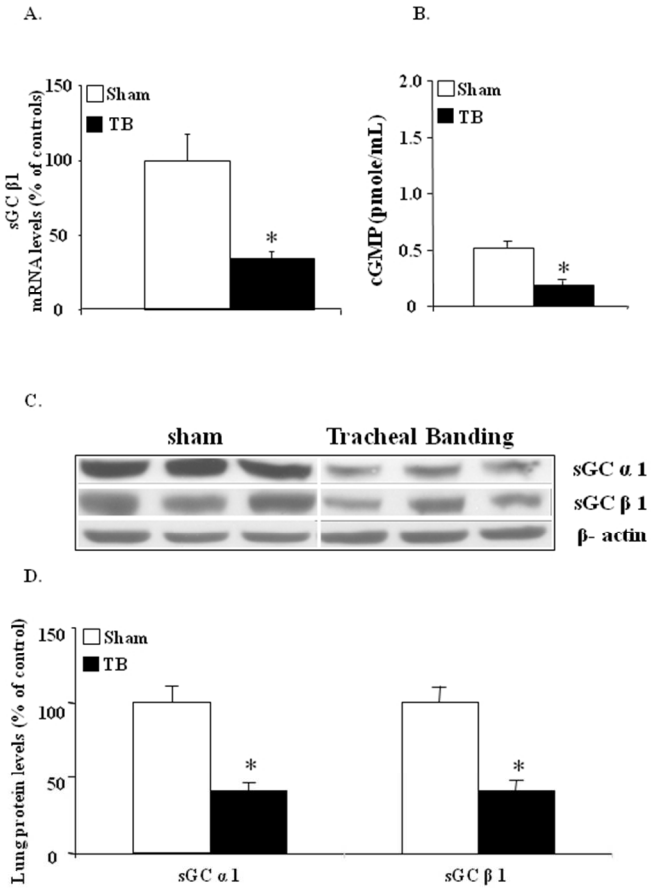

190x275mm (96 x 96 DPI)

AJRCMB Articles in Press. Published on 29-October-2014 as 10.1165/rcmb.2014-0092OC

Figure 3

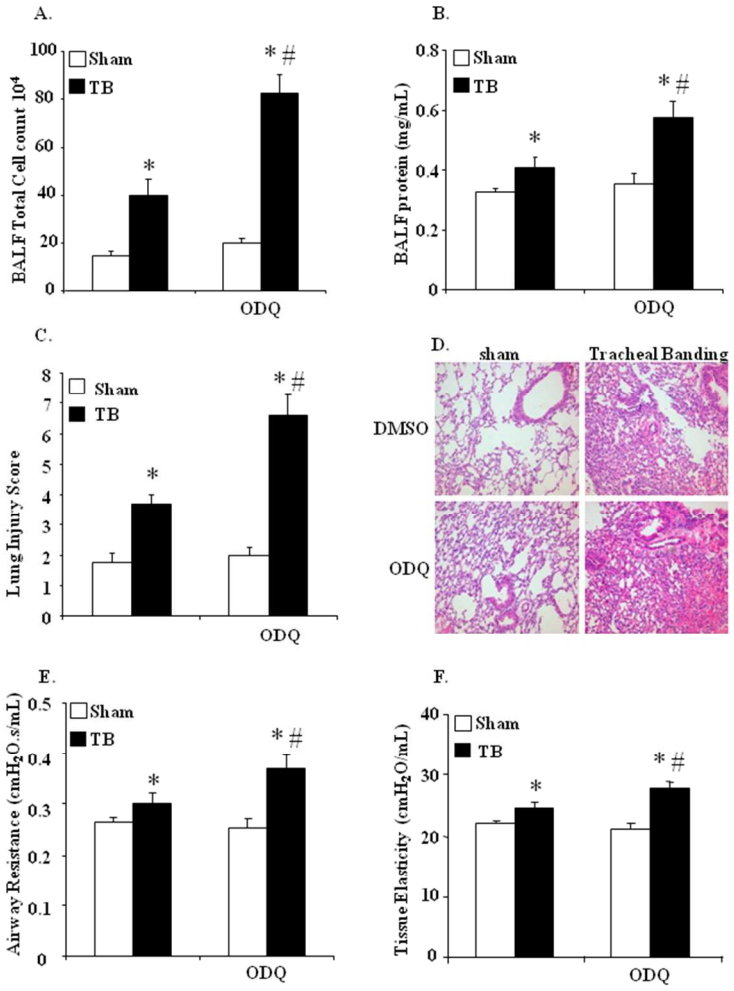

190x275mm (96 x 96 DPI)

Figure 4

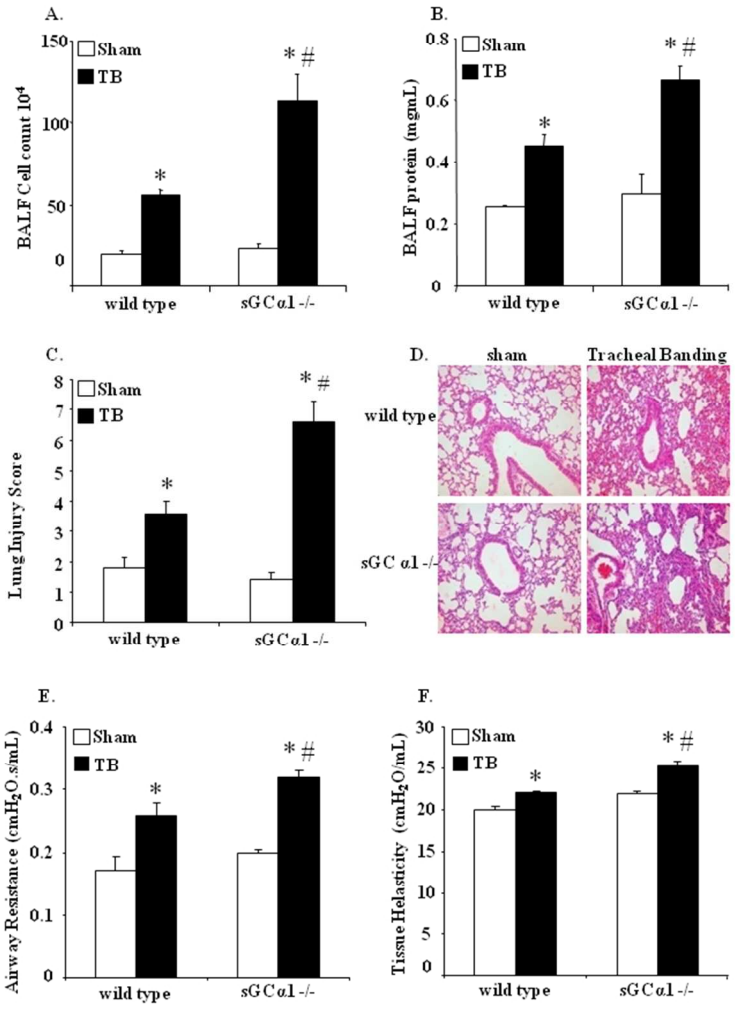

190x275mm (96 x 96 DPI)

AJRCMB Articles in Press. Published on 29-October-2014 as 10.1165/rcmb.2014-0092OC

Figure 5

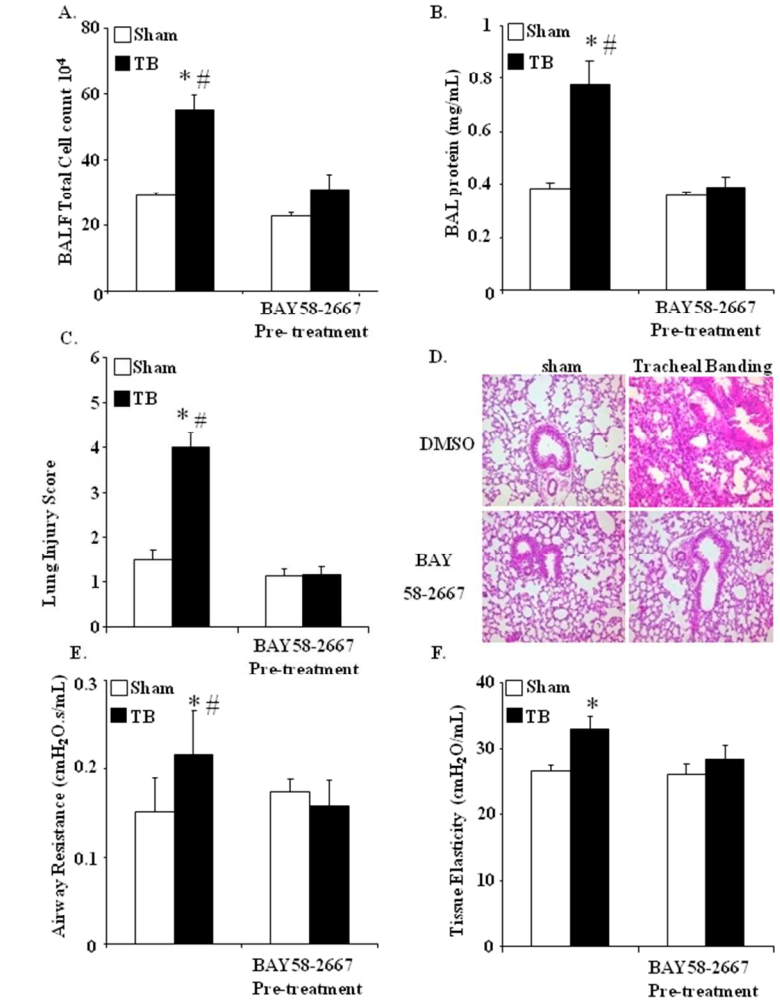

190x275mm (96 x 96 DPI)

Figure 6

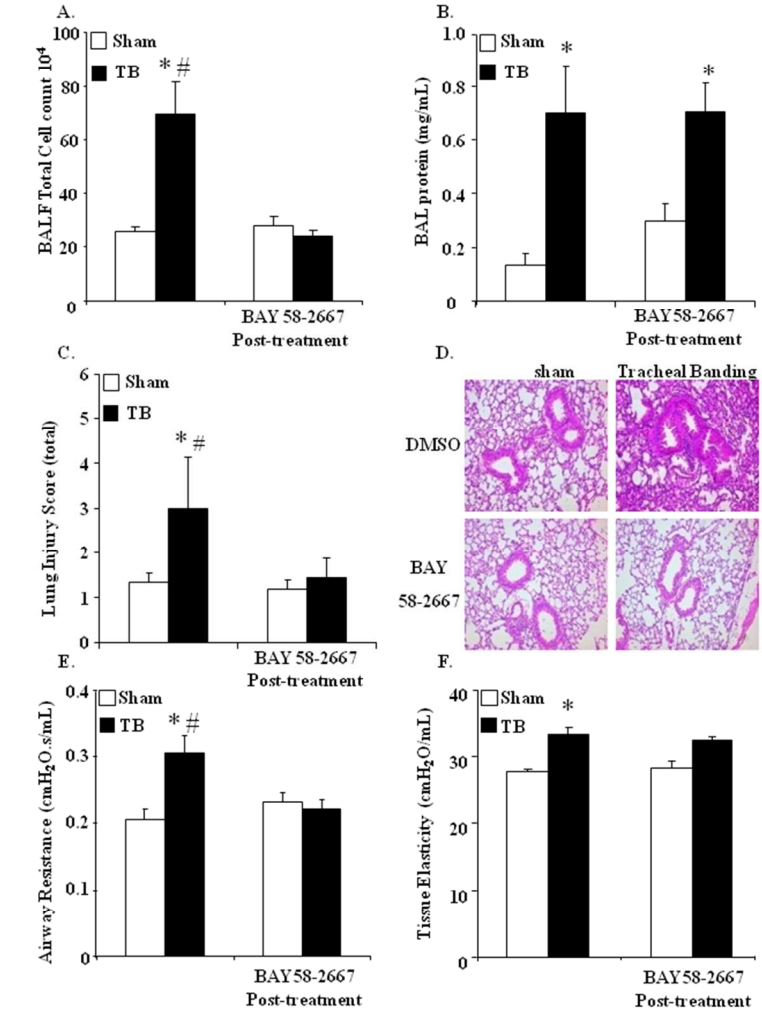

190x275mm (96 x 96 DPI)

AJRCMB Articles in Press. Published on 29-October-2014 as 10.1165/rcmb.2014-0092OC

Figure 7

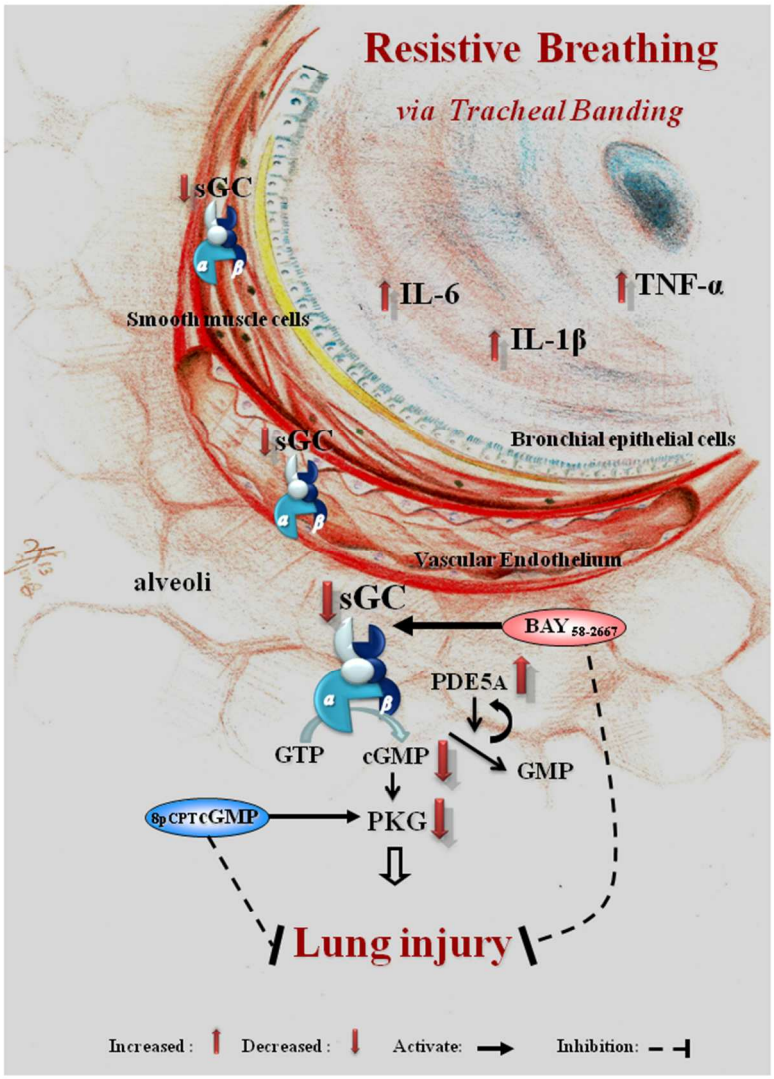

190x275mm (96 x 96 DPI)

On line data supplement

Guanylyl cyclase activation reverses resistive breathing induced lung injury and inflammation

Constantinos Glynos, Dimitris Toumpanakis, Konstantinos Loverdos, Vassiliki Karavana, Zongmin Zhou, Christina Magkou, Maria Dettoraki, Fotis Perlikos, Athanasia Pavlidou, Vasilis Kotsikoris, Stavros Topouzis, Stamatios E. Theocharis, Peter Brouckaert, Athanasios Giannis, Andreas Papapetropoulos and Theodoros Vassilakopoulos.

Methods

Reagents: Reagents for SDS-polyacrylamide gel electrophoresis and western blotting were obtained from Biorad (Hercules, CA). The Supersignal Chemiluminescent Substrate was obtained from Pierce (Rockford, Illinois). X-ray film was obtained from Eastman Kodak (Rochester, NY). Rabbit polyclonal antibodies against sGCα1 and β-actin were purchased from Sigma-Aldrich (St Luis, MO), the anti-sGCβ1 antibody was obtained from Cayman Chemicals (Ann Arbor, MI). The anti-rabbit HRP-labeled secondary antibody for western blotting was purchased from NEN Life Science Products, Inc (Boston, MA). Bronchoalveolar lavage fluid levels of tumour necrosis factor (TNF)-α, interleukin (IL)-1β, or IL-6 were measured with commercially available enzyme-linked immunosorbent assay kits (HS Quantikine; R&D Systems, Minneapolis, MN) according to the manufacturer's instructions. All other reagents, including SYBRGreen I, LPS Pseudomonas aureginosa serotype 10,

AJRCMB Articles in Press. Published on 29-October-2014 as 10.1165/rcmb.2014-0092OC

1H-[1, 2, and 4] oxodiazolo [4, 3-α] quinoxalin-l-one (ODQ), and 8pCPTcGMP were obtained from Sigma-Aldrich (St Louis, MO).

Study Design: Eight-to-twelve-week old male C57BL/6 mice, weighing 16–24 g were used were purchased from Pasteur Institute (Athens, Greece). sGCα1-/- mice were provided by the SPF facility of the Department of Molecular Biomedical Research, VIB, Ghent, Belgium. sGCα1-/- mice were generated on a mixed 129S6/Swiss background as previously described (1) and backcrossed for at least 10 generations to the C57BL/6J background (2). sGCα1-/- mice carry a targeted deletion of the sixth exon of the gene encoding sGCα1, resulting in the expression of a mutant, catalytically inactive protein. Mice were maintained in standard conditions under a 12-hour light-dark cycle, provided a standard diet and chlorinated tap water ad libitum. All procedures were in accordance to European Union Directive for care and use of laboratory animals and were approved by the Greek Veterinary Administration and the ethical committee of Evangelismos Hospital.

Tracheal Banding protocol: After general anaesthesia with intraperitoneal xylazine (5 mg/kg) and ketamine (90 mg/kg) ip, and sterile preparation, mice were placed under a visual microscope. An anterior cervical incision was made and segment of the extrathoracic trachea was exposed. The outer diameter of the trachea was measured with a calliper gauge and the area surface was calculated. The new perimeter of the trachea was calculated to provide a surface area half of the initial, by placing around the trachea a sterile nylon band of the adequate length equal to the calculated perimeter. The band was sutured firmly in place and the animal returned to cage after suturing the excision of the skin provided tracheal occlusion. Sham surgery of control mice consisted of anaesthesia, a neck incision, and tracheal dissection without banding. Animals were sacrificed 24 hrs after treatment.

Respiratory System Mechanics: The function of the respiratory system after tracheal banding was estimated with the use of the forced oscillation technique and by performing static pressure volume curves, as previously described(3). Following tracheal banding, the animals were anaesthetized with an intraperitoneal injection of ketamine (100 mg/kg) and xylazine (10 mg/kg). An anterior cervical incision was performed, the nylon band was removed and the animals were tracheostomized below the level of banding with a tracheal cannula (20G). Following, the animals were connected to a small animal ventilator (Scireq, Montreal, Canada) and ventilated with a 7 ml.kg-1 tidal volume, 150 breaths x min^{-1} and the end expiratory pressure was set to 3 cmH20. Following three minutes of ventilation, an ip injection of succinylcholine (8 mg/kg) was performed, to cease spontaneous breathing and after one minute, three forced oscillation perturbations were performed, with one minute interval, to estimate lung mechanics. A static pressure volume curves was also constructed following one minute of ventilation after the last oscillation perturbation. Results from repeated measures in every animal were averaged. Prior to measurements (30 sec) the lung volume history was once standardized by one inflation to total lung capacity, as estimated by airway opening pressure at 30 cmH20. During ventilation, the heart rate was monitored to ensure adequate depth of anaesthesia.

Forced Oscillation Technique: The forced oscillation perturbation consists of a pseudorandom waveform of low frequencies (0.5-19.75 Hz) applied for 8 seconds with a peak to peak volume of 3 ml/kg. Pressure and volume data are recorded and the impedance of the respiratory system is calculated using the Fast Fourier transformation. Impedance (Z) is then fitted to constant phase model : $Zrs(f) = Rn + i2\pi fI + (G-iH)/(2\pi f)a$, where Rn is the Newtonian resistance of the airways, i is the imaginary unit, f is the frequency, I is the inertance of the gas in the airways, G

AJRCMB Articles in Press. Published on 29-October-2014 as 10.1165/rcmb.2014-0092OC

represents tissue viscance (viscous dissipitation of energy) and H represents tissue elasticity and alpha can be calculated through the equation $\alpha = (2/\pi)\arctan(H/G)$. Data were accepted only when the Coefficient of Determination (fit of the model) was more than 0.9. Static Pressure Volume Curve: Static pressure volume curves of the respiratory system were performed by gradually inflating and deflating the lungs with a total volume of 40 ml/kg at seven steps each. The static compliance of the respiratory system was estimated by the slope of the mid linear part in the expiratory limb of the PV curve. Hysteresis (area between inspiratory and expiratory limb) was automatically calculated (FlexiVent software)(3).

Bronchoalveolar lavage fluid: Following 24 hrs of tracheal banding, the animals were sacrificed by exsanguination (vena cava dissection) following anaesthesia with ketamine (100mg/kg) and xylazine (10mg/kg) ip. After exsanguinations, the trachea was cannulated with a 20 gauge plastic catheter. Lungs were lavaged by infusing 1 mL warm saline, three sequential times. The recovered bronchoalveolar lavage fluid (BALF) was centrifuged; cells were collected and resuspended in PBS. Differential BALF cell counts were performed on Giemsa-stained cytospins and percentages of eosinophils lymphocytes, neutrophils and macrophages were determined. Protein concentration was measured in the BALF using the Lowry method, employing bovine serum albumin as a standard. TNF-α, IL-1β, and IL-6 levels were measured with ELISA from BAL fluid supernatant with the standard protocol supplied by the manufacturer (R & D systems).

Lung Histology: Following bronchoalvolar lavage, the left lung was harvested from mice and immersed in 4% formaldehyde solution. The tissue was embedded in paraffin wax, serially sectioned, and stained with hematoxylin-eosin, using standard methods. Two pathologists blinded for treatment evaluated the histopathological

findings in the lung. A scoring system to grade the degree of lung inflammation have been used based on the following histological features: (i) capillary congestion, (ii) intra-alveolar haemorrhage, (iii) interstitial neutrophil infiltration, (iv) intra-alveolar neutrophil infiltration, (v) focal thickening of alveolar membranes. A scale from 0 to 3 for each feature will be used (0: absence, 1: mild, 2: moderate, 3: most severe) (4).

cGMP measurements: To determine whether RB effect on sGC activity we measured cGMP production in BALF collected 24hrs after tracheal banding. Cells were pelleted, washed twice, and incubated in Hanks' balanced salt solution for 15 min; cells were then lysed with 0.1 N HCl, and cGMP levels were analyzed in the extracts using a commercially available enzyme immunoassay kit following the manufacturer's instructions (Direct cGMP Elisa Kit; Enzo Life Sciences, Lausen, Switzerland).

Quantitative real-time PCR: Quantitative real-time PCR: Total cellular RNA was isolated using the Rneasy Mini Kit isolation method (Qiagen) and quantified on a NanoDrop 2000 (Thermo Scientific). 500ng of total RNA reverse transcribed with the PrimeScript RT Reagent Kit (Takara). Real time PCR amplification performed with the KAPA SYBR Fast One-step qRT-PCR protocol (KapaBiosystems). Amplification and Real-Time fluorescence detection performed using the Rotor Gene 6000 (Corbett). PCR amplifications were performed in triplicate. Primer sequences were as follows: sGCα1 subunit: sense, 5'-CGG AAA ATC AAT GTC AGC CC-3', antisense, 5'-AGG GAA GTT TGG TGG AAG CTC-3', sGCβ1 subunit: sense, 5'-GCG GTA CTC TTG CCT GGA AG-3', antisense, 5'-GACCATAATTGCGGATCACCA-3', 18SrRNA: sense, 5'-GTAACCCGTTGAACCCCATT-3', antisense: 5'-CATCCAATCGGTAGTAGCG-3', GAPDH: sense, 5'- ACC-ATC-TTC-CAG-GAG-CGA-GAC-3', antisense, 5'-

AJRCMB Articles in Press. Published on 29-October-2014 as 10.1165/rcmb.2014-0092OC

GCC-TCC-TCC-ATG-GTG-GTG-AA-3'. Reaction samples had a final volume of 20 μL. Amplification conditions consisted of 30 seconds at 95°C, followed by 35 cycles of: 3 seconds at 95°C, 20 seconds at 59°C, 2 seconds at 72°C. 18S and GAPDH amplification was used as the endogenous control. Ct values were automatically calculated by the machine's software and normalized to the endogenous control gene by using the $2^{-\Delta\Delta C_T}$ method (5)

Immunoblot analysis of sGC subunits: After sacrificing the mice, lung tissue was frozen in liquid nitrogen and stored at –80 °C until used. One lobe was homogenized in 10 volumes (w/v) of a lysis buffer containing 1% Triton-X, 1% SDS, 150mM NaCl, 50mM NaF, 1mM Na3VO4, 0.5% sodium deoxycholate, 1mM EDTA, 0,1mM EGTA and protease inhibitors (10 μg/ml aprotinin, 10 μg/ml pepstatin, and 20 mM PMSF). Samples were subjected to SDS-PAGE followed by blotting with antibodies against the α1 (1:5,000) or β1 (1:2,000) and visualized using a chemiluminescent substrate. Values obtained for the α1 and β1 sGC subunit were normalized for actin and presented as % of control (6-8).

ODQ treatment: C57BL/6 mice were treated with inhaled ODQ (1H-[1, 2, 4] oxodiazolo [4, 3-] quinoxalin-l-one) or vehicle (inhaled DMSO 10 %.), 30 min before tracheal banding. The ODQ (5 mg ODQ diluted in 50μL DMSO and then further dissolved in 5 ml saline) and the vehicle were administered over a 20-minute period in a nebulisation chamber under continuous oxygen flow, 30 minutes prior to tracheal banding. Animals were sacrificed 24 hrs after treatment.

8pCPT cGMP treatment: C57BL/6 mice were treated with inhaled 8pCPT cGMP or vehicle (inhaled DMSO 10 %.), 30 min before tracheal banding. The 8pCPT cGMP (10 mg 8pCPT cGMP diluted in 50μL DMSO and then further dissolved in 5 ml

saline) and the vehicle were administered over a 20-minute period in a nebulisation chamber under continuous oxygen flow, 30 minutes prior to tracheal banding. Animals were sacrificed 24 hrs after treatment.

BAY 58-2667 treatment: In the pharmacological experiment of RB, C57BL/6 mice were treated with the sGC activator BAY 58-2667 (4-[((4-carboxybutyl) {2-[(4-phenethylbenzyl) oxy] phenethyl} amino) methyl [benzoic] acid) (10 μg/kg, i.p.) or vehicle (DMSO 10%, i.p.). BAY58-2667 was synthesized as previously described(9). Prophylactic protocol: wild type C57BL/6 mice were treated with the sGC activator BAY 58-2667 (10μg/kg, i.p.) 30 min before tracheal banding. Mice were sacrificed 24 hrs after tracheal banding. Therapeutic protocol: mice were treated with the sGC activator BAY 58-2667 (10μg/kg, i.p.) 24 hrs after tracheal banding. Mice were sacrificed 30 hrs after tracheal banding.

Statistical Analysis. Results are presented as means± SEM of the number of observations. Statistical analysis was performed with Sigma Stat software (SPSS 11.5, Chicago, IL, USA) using nonparametric tests for continuous variables (Kruskall-Wallis, Mann-Whitney U). Differences were considered significant when $p<0.05$.

Figure Legends

Figure E1: The murine model of tracheal banding. **A.** After general anesthesia mice were placed under a visual microscope and an anterior cervical incision was made for trachea dissection. **B.** After the dissection, the extrathoracic segment of the trachea was exposed for perimeter calculation. **C.** The outer diameter of the trachea was

AJRCMB Articles in Press. Published on 29-October-2014 as 10.1165/rcmb.2014-0092OC

measured with a caliper gauge and the area surface was calculated. A new perimeter of the trachea has been calculated to provide a surface area half of the initial. **D.** A sterile nylon band of the adequate length equal to the calculated perimeter was placed around the trachea. **E.** and **F**. The band was sutured firmly in place to provide tracheal occlusion. The animal returned to cage after suturing the excision of the skin.

Figure E2: Protein levels for the Phosphodiesterase (PDE)-5A are increased in the lungs of TB mice. Protein levels of the PDE5A were increased in mice after 24 hrs of resistive breathing. Sham operated (control) or TB (TB) mice were sacrificed 24hrs after treatment. Representative western blots for the PDE5A and β-actin. Blots were quantified by densitometry. Expression for each subunit normalized for β-actin was set at 100% for sham operated mice. Values are expressed as means ± SEM; n=5; *p< 0.05 from sham operated (control) group.

Figure E3: ***Restoration of sGC downstream signalling: PKG activation attenuates lung injury caused by tracheal banding***. To elucidate whether the restoration of sGC downstream signalling protects from the RB induced-lung injury, 8pCPTcGMP, a cell-membrane permeable analogue of cGMP, was administered by nebulisation 30min prior to RB **A.** Exposure of animals to the nebulised 8pCPTcGMP, partially, reversed the effect of tracheal banding by reducing BALF inflammatory cell number. **B.** 8pCPTcGMP inhalation attenuated the effect of tracheal banding on albumin leakage. **C.** Lung histological evaluation by light microscopy revealed the attenuation of inflammation and neutrophil infiltration in mice treated with 8pCPTcGMP. Inhalation of 8pCPTcGMP decreased interstitial and intraalveolar infiltration and focal congestion in the lung tissue, compared to the group of TB (TB) mice. **D.** Representative histological section stained with hematoxylin-eosin of quietly breathing (control) and TB (TB) mice, with or without exposure to 8pCPTcGMP,

respectively. Note that intralveolar and interstitial infiltration of inflammatory cells, focal thickening and capillary congestion that occurs following tracheal banding, is attenuated after 8pCPTcGMP inhalation. **E.** Elevated tissue elasticity, following tracheal banding, was attenuated after inhalation of PKG activator **F.** The decrease of the static compliance of the respiratory system, 24hs after tracheal banding was reversed after inhalation of PKG activator. Values are expressed as means ± SEM; n=10; *p< 0.05 from sham operated (control) group and # p<0.05 from TB group.

Figure E4: ***PKG activation attenuates the increase in cytokines caused by tracheal banding.*** **A.** Tracheal banding increases BALF levels of TNF-α whereas 8pCPTcGMP inhalation attenuated TNF-α levels. **B.** BALF levels of IL-6 were increased after tracheal banding compared to sham operated mice. Inhalation of 8pCPTcGMP reduced Il-6 levels in the BAL fluid. **C.** BALF levels of IL-1β were increased after tracheal banding, whereas 8pCPTcGMP inhalation attenuated lung inflammation by reducing levels of IL-1β. Values are expressed as means ± SEM; n=10; *p< 0.05 from sham operated (control) group and # p<0.05 from TB group.

Figure E5: **BAY 58-2667 reversed the RB-induced attenuation of cGMP levels.** Cyclic guanosine monophosphate (cGMP) levels in bronchoalveolar lavage (BAL) were attenuated 24 hrs after tracheal banding. **A.** Prophylactic and **B.** therapeutic administration of BAY 58-2667 reversed the RB-induced attenuation of cGMP levels. Values are expressed as means ± SEM; n=10; *p< 0.05 from sham operated (control) group.

Figure E6: Schematic overview of the tracheal banding protocols: **A.** Pretreatment of mice with ODQ. Inhaled ODQ was administrated 30min prior to tracheal banding Animals were sacrificed 24 hrs after treatment **B.** Pretreatment of mice with 8pCPT

AJRCMB Articles in Press. Published on 29-October-2014 as 10.1165/rcmb.2014-0092OC

cGMP. Inhaled 8pCPT cGMP was administrated 30min prior to tracheal banding. Animals were sacrificed 24 hrs after treatment **C.** Prophylactic treatment with BAY 58-2667. Administration (i.p.) of BAY 58-2667, 30min prior to tracheal banding. Animals were sacrificed 24 hrs after treatment **D.** Therapeutic treatment with BAY 58-2667. Administration (i.p.) of BAY 58-2667, 24hrs after tracheal banding. Animals were sacrificed 30 hrs after treatment.

Reference List

1. Buys ES, Sips P, Vermeersch P, Raher MJ, Rogge E, Ichinose F, Dewerchin M, Bloch KD, Janssens S, Brouckaert P. Gender-Specific Hypertension and Responsiveness to Nitric Oxide in SGCalpha1 Knockout Mice. *Cardiovasc Res* 2008;79:179-186.

2. Buys ES, Cauwels A, Raher MJ, Passeri JJ, Hobai I, Cawley SM, Rauwerdink KM, Thibault H, Sips PY, Thoonen R, et al. SGC(Alpha)1(Beta)1 Attenuates Cardiac Dysfunction and Mortality in Murine Inflammatory Shock Models. *Am J Physiol Heart Circ Physiol* 2009;297:H654-H663.

3. Toumpanakis D, Kastis GA, Zacharatos P, Sigala I, Michailidou T, Kouvela M, Glynos C, Divangahi M, Roussos C, Theocharis SE, et al. Inspiratory Resistive Breathing Induces Acute Lung Injury. *Am J Respir Crit Care Med* 2010;182:1129-1136.

4. Murao Y, Loomis W, Wolf P, Hoyt DB, Junger WG. Effect of Dose of Hypertonic Saline on Its Potential to Prevent Lung Tissue Damage in a Mouse Model of Hemorrhagic Shock. *Shock* 2003;20:29-34.

5. Schmittgen TD, Livak KJ. Analyzing Real-Time PCR Data by the Comparative C(T) Method. *Nat Protoc* 2008;3:1101-1108.

6. Glynos C, Kotanidou A, Orfanos SE, Zhou Z, Simoes DC, Magkou C, Roussos C, Papapetropoulos A. Soluble Guanylyl Cyclase Expression Is Reduced in LPS-Induced Lung Injury. *Am J Physiol Regul Integr Comp Physiol* 2007;292:R1448-R1455.

7. Glynos C, Dupont LL, Vassilakopoulos T, Papapetropoulos A, Brouckaert P, Giannis A, Joos GF, Bracke KR, Brusselle GG. The Role of Soluble Guanylyl Cyclase in Chronic Obstructive Pulmonary Disease. *Am J Respir Crit Care Med* 2013;188:789-799.

8. Papapetropoulos A, Simoes DC, Xanthou G, Roussos C, Gratziou C. Soluble Guanylyl Cyclase Expression Is Reduced in Allergic Asthma. *Am J Physiol Lung Cell Mol Physiol* 2006;290:L179-L184.

9. von Wantoch RM, Kumar V, Zhou Z, Moschner J, Marazioti A, Bantzi M, Spyroulias GA, van den Akker F, Giannis A, Papapetropoulos A. Insights into Soluble Guanylyl Cyclase Activation Derived From Improved Heme-Mimetics. *J Med Chem* 2013.

AJRCMB Articles in Press. Published on 29-October-2014 as 10.1165/rcmb.2014-0092OC

Figure E1

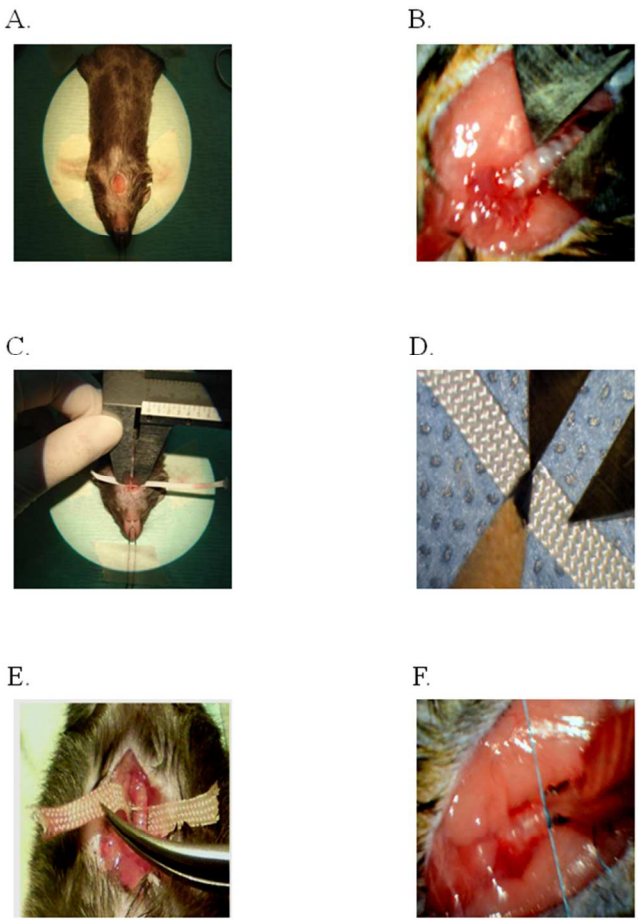

190x275mm (96 x 96 DPI)

Figure E2

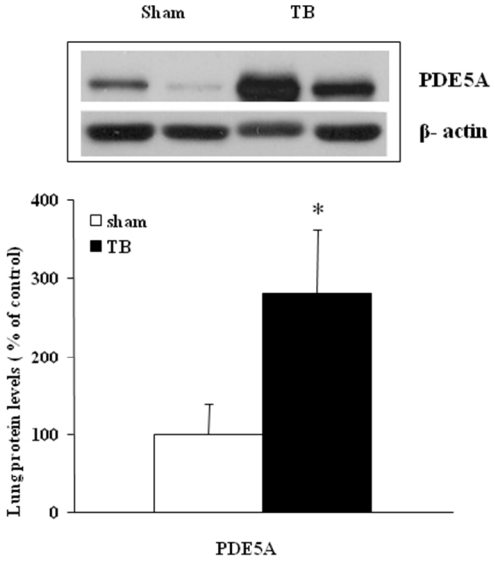

190x275mm (96 x 96 DPI)

AJRCMB Articles in Press. Published on 29-October-2014 as 10.1165/rcmb.2014-0092OC

Figure E3

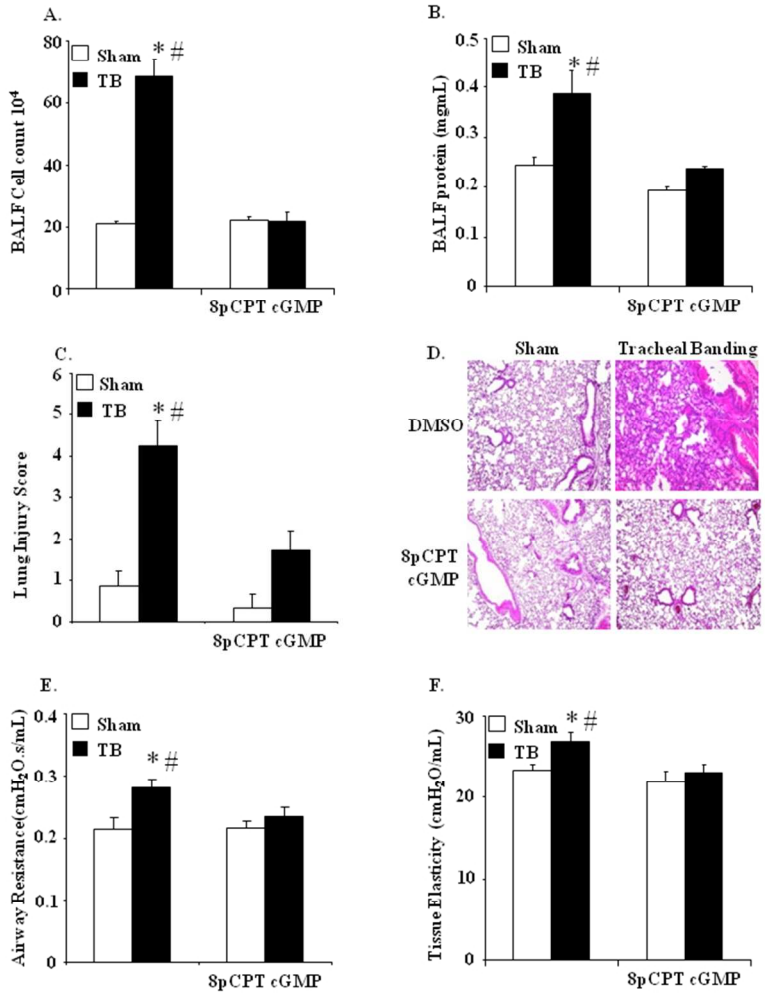

190x275mm (96 x 96 DPI)

Figure E4

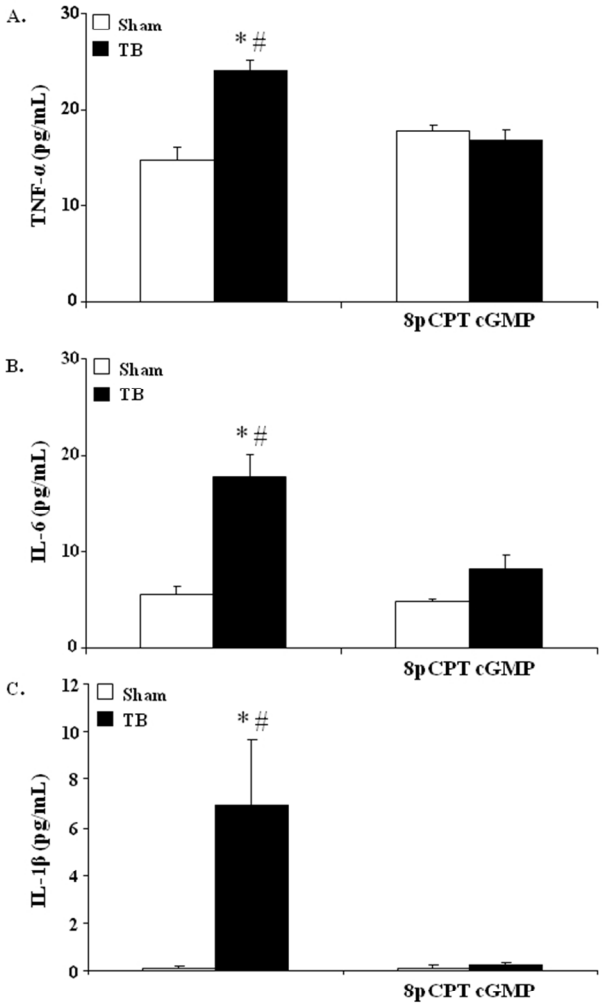

190x275mm (96 x 96 DPI)

AJRCMB Articles in Press. Published on 29-October-2014 as 10.1165/rcmb.2014-0092OC

Figure E5

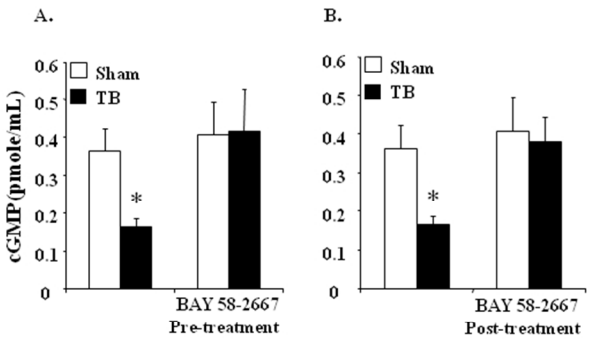

190x275mm (96 x 96 DPI)

Figure E6

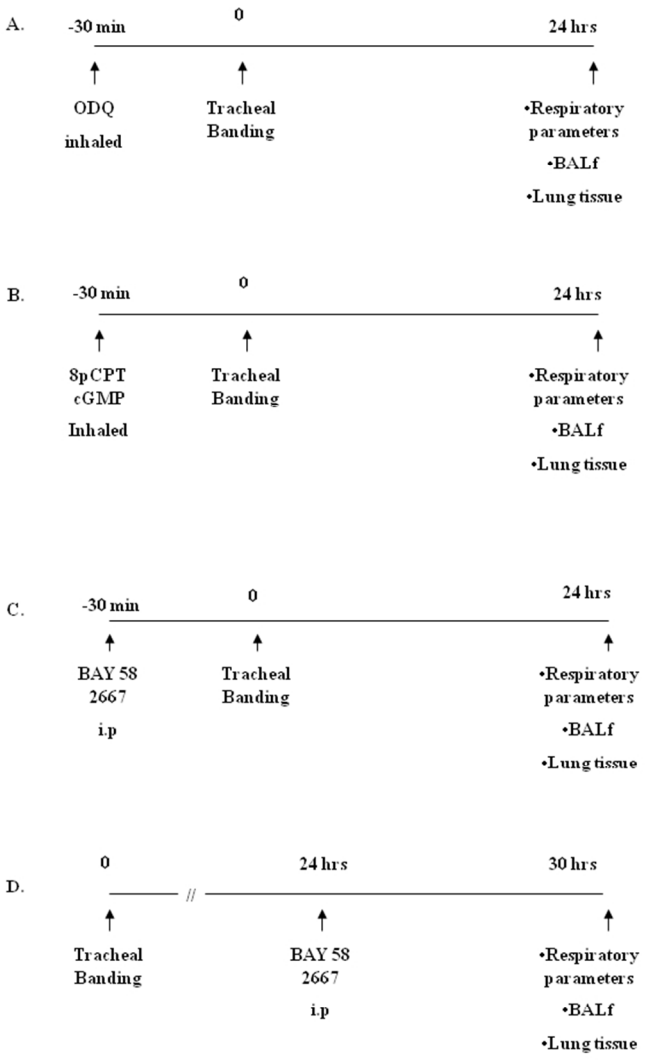

190x275mm (96 x 96 DPI)